Published online 6 October 2009 *Nucleic Acids Research, 2009, Vol. 37, No. 22* ***7533–7545***
doi:10.1093/nar/gkp812

Expanded RNA-binding activities of mammalian Argonaute 2

Grace S. Tan[1], Barry G. Garchow[1], Xuhang Liu[2], Jennifer Yeung[1], John P. Morris IV[3], Trinna L. Cuellar[3], Michael T. McManus[3] and Marianthi Kiriakidou[1,*]

[1]Department of Medicine, [2]Department of Pathology and Laboratory Medicine, University of Pennsylvania School of Medicine, Philadelphia, PA 19104, USA and [3]Department of Microbiology and Immunology, Diabetes Center, University of California, San Francisco, CA 94122, USA

Received April 28, 2009; Revised September 14, 2009; Accepted September 15, 2009

ABSTRACT

Mammalian Argonaute 2 (Ago2) protein associates with microRNAs (miRNAs) or small interfering RNAs (siRNAs) forming RNA-induced silencing complexes (RISCs/miRNPs). In the present work, we characterize the RNA-binding and nucleolytic activity of recombinant mouse Ago2. Our studies show that recombinant mouse Ago2 binds efficiently to miRNAs forming active RISC. Surprisingly, we find that recombinant mouse Ago2 forms active RISC using pre-miRNAs or long unstructured single stranded RNAs as guides. Furthermore, we demonstrate that, *in vivo*, endogenous human Ago2 binds directly to pre-miRNAs independently of Dicer, and that Ago2:pre-miRNA complexes are found both in the cytoplasm and in the nucleus of human cells.

INTRODUCTION

MicroRNAs (miRNAs) associate with proteins of the Ago family forming ribonucleoprotein complexes (miRNPs or RISCs) that regulate gene expression at transcriptional or post-transcriptional level (1–6). miRNAs are derived from endogenously encoded genes, some of which are found in clusters, in inter or intragenic regions of protein coding genes (7). miRNAs are transcribed by RNA polymerase II or III into primary microRNAs (pri-miRNAs). Most pri-miRNAs are processed in the nucleus by the ribonuclease III (RNAseIII) enzyme Drosha and Drosha's partner, the double stranded RNA-binding (dsRBD) DiGeorge syndrome critical region gene 8 protein (DGCR8 or Pasha) into 65–75 nucleotide (nt), hairpin structured pre-mature microRNAs (pre-miRNAs) (7–10).

Exportin-5 mediates transport of pre-miRNAs to the cytoplasm (11–14) where they encounter Dicer, another RNAseIII protein. Human Dicer, like Drosha, associates with RNA-binding proteins, namely human immunodeficiency virus 1 (HIV-1) transactivating response (TAR) RNA-binding protein (TRBP) and protein activator of PKR (PACT) (15,16). Recombinant human Dicer can process synthetic pre-miRNAs or long double stranded RNA duplexes *in vitro* (17,18). Dicer binds directly to Ago proteins (19) and interestingly, this interaction inhibits the RNAse activity of Dicer *in vitro*, in a dose dependent manner (19).

In mammals, after Dicer processing of pre-miRNAs, mature single stranded miRNAs assemble into miRNPs containing any of the four mammalian Ago proteins, Ago1–4. Ago2 is the only human Ago protein endowed with nuclease activity, despite remarkable homology that extends to the PIWI domains among all four human Agos (20).

In the present work, we studied the RNA binding and cleavage activities of recombinant mouse Ago2. We demonstrate that, like endogenous Ago2, mouse recombinant GST-Ago2 forms active RISC complexes *in vitro*, by binding efficiently to 22 nt RNAs. Surprisingly, our studies also show that GST-Ago2 assembles into cleavage-active complexes with pre-miRNAs and RNAs longer than 22 nt. Furthermore, we demonstrate direct association of endogenous Ago2 with endogenous pre-miRNAs in the nucleus and cytoplasm of human cells.

MATERIALS AND METHODS

Expression and Purification of GST-Ago2 and GST-D669A

The full-length coding region of mouse Ago2 (nucleotides 28–2610 of NM_153178) was amplified by PCR and subcloned into pFASTBAC-GST. The Ago2-D669A mutation was generated by substituting A2036C via Quickchange mutagenesis (Stratagene), resulting in the following codon change: GAT to GCT. The presence of the mutation was confirmed by DNA sequence analysis. Bacmid DNA was transfected into Sf9 cells for virus stock generation. For protein productions, 1×10^6 Sf9 cells/ml

*To whom correspondence should be addressed. Tel: +1 215 573 6639; Fax: +1 215 573 7599; Email: kiriakim@uphs.upenn.edu

of Sf900-II medium (Invitrogen) were infected with viruses for the wild-type Ago2 and Ago2-D669A proteins respectively, at an MOI of 1. For protein purification, 500 ml cell pellets were resuspended in 40 ml of cold buffer A containing 20 mM Tris–HCl (pH 7.5), 2 mM EDTA and 1 M NaCl with protease inhibitors (BMB #11697498001) and sonicated 6 × 10 s at 60% amplitude, on ice. Cell lysates were centrifuged and supernatants were incubated with 4 ml of pre-washed glutathione sepharose 4B beads (GE 27-4574-01) at 4°C overnight. The beads were then washed several times with buffer A-1 (buffer A, containing 2M NaCl and 0.5% Triton X-100). Subsequently, GST-Ago2 or GST-D669A protein was eluted, using 200 mM glutathione in 200 mM Tris–HCl (pH 8.0) at room temperature for 15 min and dialyzed against buffer D containing 20 mM Hepes–KOH (pH 7.9), 100 mM KCl, 0.2 mM EDTA and 0.5 mM DTT. Proteins were then subjected to anion exchange chromatography.

5′- and 3′-end labeling of RNAs

RNA oligos (or RNA isolated from immunoprecipitated Ago) were either 5′- or 3′-end radiolabeled with T4 polynucleotide kinase (NEB) or T4 RNA ligase (Ambion) respectively, as previously described (21,22).

GST-Ago2 Cleavage assays

Cleavage assays were performed as previously described (25). A total of 15 nM GST-Ago2 or GST-D669A was pre-incubated with 0.02–0.2 μM 5′P-miRNA at 37°C for 30 min, before addition of 13.6 nmol 5′-^{32}P radiolabeled target and incubation for additional 60 min. Gel extracted pre-miR-30a was heated at 95°C for 3 min, then at 65°C for 10 min and at 37°C for 30 min in RNA annealing buffer (0.1 M NaCl, 10 mM Tris–HCl pH 7.4, 1 mM EDTA), prior to use in cleavage assays. Cleavage products were analyzed on 15% Urea PAGE and detected by autoradiography. Two different radiolabeled size markers were used: (M) pBR322/MspI (NEB N3032S), and (M1) Decade RNA marker (Ambion AM7778).

Electrophoretic mobility shift assay

A total of 10.8 nM 5′-^{32}P–let-7a was incubated with increasing concentrations (3–300 nM) of GST-Ago2 or GST-D669A in a 10 μl reaction containing 5 mM DTT, 0.1 mg/ml BSA, 3% (w/v) Ficoll-400 and 5% (v/v) glycerol at 37°C for 30 min. RNA-protein complexes were then analyzed on 5.25% native polyacrylamide (37.5:1) gel containing 0.5× TBE and 1.5 mM $MgCl_2$, detected by storage phosphor autoradiography and quantified using Image Quant V1.2. Results were analyzed using Prism software (GraphPad Prism for Windows, GraphPad Software, San Diego California USA).

Pre-miRNA processing assays

5′-^{32}P-radiolabeled pre-miRNA (15 000 c.p.m.) was incubated with 15 nM GST-Ago2 protein or 0.05 U of Dicer (Ambion AM2212) in a 10 μl reaction containing 1× microRNA buffer (MIB: 40 mM KOAc, 2 mM $MgCl_2$ and 1 mM DTT) and 40 U Recombinant Ribonuclease inhibitor (RNAsin, Promega N2515) at 37°C for 60 min. Reaction products were analyzed on 15% Urea PAGE and detected by autoradiography. For reconstitution experiments, radiolabeling of target TD and cleavage assays were performed as described above, with the following modifications: 15 nM of GST-Ago2 or GST-D669A and/or Dicer (0.05 U) was pre-incubated with 20–200 nM 5′P–pre-let-7a-3 at 37°C for 60 min.

UV Photo-crosslinking

A total of 2000 c.p.m. of 3′-^{32}P pCp labeled 5′P–let-7a, let-7a, 5′P–pre-let-7a-3, pre-let-7a-3 or 5′P–73 nt single stranded RNA was incubated with ~16.7 nM of recombinant Dicer-free GST-Ago2 in 10 μl of 1× MIB at 37°C for 30 min, before irradiation with 254 nM UV light for 60 min on ice (UVLMS-38 EL Series 3UV Lamp). Photo-crosslinked samples were then analyzed on 1.0 mm 4–12% NuPAGE (Invitrogen NP0323) and detected by storage phosphor autoradiography. In competition experiments 10×, 50×, and 100× molar excess of the same but unlabeled RNA oligos or unlabeled yeast tRNA (Invitrogen 15401011) were included.

Preparation of immortalized MEF cell lines and cell culture

The inducible Dicer-null mouse embryonic fibroblasts (MEFs) were derived from mouse embryos that are either heterozygous or homozygous for a targeted allele of *dicer* with the second RNaseIII domain flanked by loxP sites (23) and are hemizygous at the Rosa 26 allele for a cre-conditional YFP reporter gene and a tamoxifen inducible CreERT fusion protein. The primary MEFs were harvested and processed from the inducible Dicer-null mouse embryos between E12.5 and E14.5. They were then immortalized by co-transfection with a SV40 construct and a puromycin expression vector at Passage 2 and selected in 2 μg/ml puromycin. The immortalized MEFs were cultured in DMEM supplemented with 10% Fetal Bovine Serum and 2 mM L-Glutamine. To induce the recombination of loxP sites and depletion of Dicer, 50 nM of 4-hydroxytamoxifen (4-OHT) was added to the medium for 4 days. Then, 4-OHT was removed and the MEFs were cultured for additional 4–6 days before they were collected, snap frozen in liquid nitrogen and stored at −80°C.

Immunofluorescence microscopy

HeLa cells were grown on autoclaved glass coverslips in six-well plates to 40 % confluency, washed with 1× PBS and fixed with 2 % formaldehyde in 1× PBS at room temperature (RT) for 10 min. The cells were then washed 3× 1 min with 1× PBS, permeabilized with buffer containing 0.5% Triton X-100 in 1× PBS at RT for 5 min, and washed again with 1× PBS before incubation with Ago2 antibody (Wako, Clone #4G8, 1:75 dilution) or cytoplasmic β-tubulin antibody (Developmental studies hybridoma bank, E7 ascites, 1:1000 dilution) overnight at 4°C. After 3× 10 min washes with gentle agitation in

2% BSA in 1× PBS, cells were incubated with goat anti-mouse Alexa 488 secondary antibody (Molecular Probes #A11017, 1:1000 dilution) at RT for 45 min. After three washes with 1× PBS, ProLong Gold antifade mounting medium with DAPI (Molecular Probes #P36931) was added to the cells, prior to fixing onto glass slides. Immunofluorescence images were captured using Deltavision Spectris Deconvolution Microscope (Applied Precision, Inc., Issaquah, WA) with a 60×, 1.42 NA oil immersion lens (Olympus #PLAPON 60XO) and deconvoluted with its accompanying softWoRx software. The images were then adjusted using Image J (NIH) program.

Nuclear-cytoplasmic fractionation

HeLa cells (~60×10^6 for each experiment) were harvested without trypsin and pelleted at $500 \times g$ for 5 min. Nuclear and cytoplasmic fractionations were performed with ProteoJET™ Cytoplasmic and Nuclear Protein Extraction Kit (Fermentas #K0311) as per manufacturer's protocol. Western blot analyses were performed on 25 ng of protein from each extract using antibodies against Lamin A/C (Santa Cruz, sc-7292 1 : 100 dilution) and endoplasmic reticulum (ER)- associated calnexin (Cell Signaling # 2433, 1 : 1000 dilution) to determine efficiency of nuclear fractionation, cytoplasmic β-tubulin (Developmental studies hybridoma bank, E7 ascites, 1 : 2000 dilution), and human Ago2 (Wako, Clone # 4G8, 1 : 200 dilution) as indicated in figures.

Immunoprecipitation and northern blotting

HeLa cell lysates were incubated with ~80 µl of protein G agarose beads pre-bound to 10 µl of anti-human Ago2 antibody (Wako, Clone # 4G8) or 5 µl of non-immune mouse serum at 4°C overnight. Agarose beads were then washed copiously with 1% Empigen BB (Fluka 45165) in RSB-200 [20 mM Tris (pH 7.5), 200 mM NaCl, 2.5 mM $MgCl_2$]. A 10% total of protein G agarose volume was used for western blots, 45% for pre-miRNA processing assays and 45% for Ago2-bound RNA isolation. RNA was isolated from the beads as described previously (21). The aqueous phase was treated with 10 U of Turbo DNase (Ambion AM2238) at 37°C for 15 min prior to phenol/chloroform/isoamyl alcohol extraction and RNA precipitation. Northern blot analysis was performed as described previously (21). Equal amounts of RNA (~200 ng) per sample were loaded. The membranes were probed with 5′-^{32}P-radiolabeled LNA-miR-21 or LNA-let-7a probe at 45°C overnight, washed and miRNA/pre-miRNA signals were detected by storage phosphor autoradiography.

Synthetic RNAs

let-7a-3
5′p-UGAGGUAGUAGGUUGUAUAGUU-3′

Pre-let-7a
5′p-UGAGGUAGUAGGUUGUAUAGUUUGGGGC
UCUGCCCUGCUAUGGGAUAACUAUACAAUCU
ACUGUCUUUCC-3′

Target TD
5′-UAUACAACCUACUACCUCAUC-3′

73 nt RNA
5′p-ACGAGAUUGAACGUUGAGGUAACGUUCCC
GCCCGUUAAUUGGUGGCCUCUAUCUAGACCA
GAGCUCAGAAGAA-3′

Target TL
5′p-GGUUAUGACGUGCAUGGUGUUAAUUGGU
AUCAACCACUAUACAACCUACUACCUCAACGU
UCAAUCUCGUAUGCGUAAAGUGCUAAGUGCA
UGGAUGCGA-3′

Pre-miR-30a
5′p-UGUAAACAUCCUCGACUGGAAGCUGUGAA
GCCACAGAUGGGCUUUCAGUCGGAUGUUUGC
AGC-3′

miR-30a
5′p -UGUAAACAUCCUCGACUGGAAGCU-3′

Target TGS
5′-AACCUGCUUCCAGUCGAGGAUGUUUACACC
AAG-3′

LNA-miR-21
5′-TCAACATCAGTCTGATAAGCTA-3′

LNA-let-7a-3
5′p-AACTATACAACCTACTACCTCA-3′a

PML-GL3
5′-UCGAAGUACUCAGCGUAAGUGGCUGUGAA
GCCACAGAUGGGCCACUUACGGAGUACUUUG
AGC-3′

RESULTS

Expression and purification of wild-type and catalytically inactive mouse Ago2

Our initial objective was to study the *in vitro* reconstitution of mammalian RISC loading complex (RLC). Wild-type glutathione-S-transferase (GST) tagged mouse Argonaute 2 (GST-Ago2) was expressed in Sf9 insect cells infected with baculovirus. Human and mouse Ago2 proteins share extensive sequence similarity (99% identity, by CLUSTALW2 of mouse—NP_694818- and human—NP_036286-Ago2). Although studies with recombinant mouse Ago2 have not been reported, the DDH sequence within the P-element induced wimpy testis (PIWI) domain to which the catalytic activity of human Ago2 has been ascribed (20) is also present in mouse Ago2. We therefore expressed catalytically inactive mouse GST-Ago2 in Sf9 cells by substituting the aspartate at position 669 with alanine (mutant GST-D669A). Batch protein purification with GST resin was followed by elution with glutathione and anion exchange chromatography, yielding proteins of high purity. Coomassie-stained NuPAGE gels of GST-Ago2 and GST-D669A, as well as mass spectrometric analysis

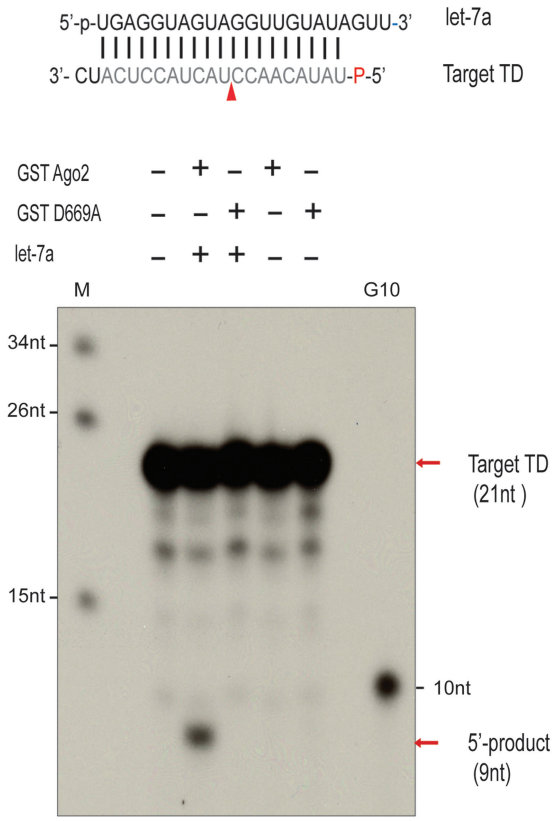

Figure 1. Recombinant mouse GST-Ago2 and let-7a form active RISC *in vitro*. 15 nM of either wild-type or catalytically inactive (D669A) GST-Ago2 was loaded with 0.02 μM synthetic 5′P-let-7a and then incubated with 13.6 nmol 5′-^{32}P target RNA (TD). Reactions were analyzed by 15% Urea PAGE and detected by autoradiography. pBR322/MspI DNA marker (M) and a synthetic 10 nt oligo (G10) were radiolabeled and included as size markers.

results, are shown in Supplementary Figure S1. To test the activity of GST-Ago2, the protein was first loaded with synthetic 5′-phosphorylated let-7a. The resulting GST-Ago2:let-7a complex was then incubated with a 21 nt 5′-^{32}P-radiolabeled RNA target (TD) complementary to let-7a. As shown in Figure 1, GST-Ago2:let-7a, but not the catalytically inactive GST-D669A:let-7a, cleaved the target TD.

RNA-binding kinetics of recombinant Ago2 and D669A

Next, we tested the RNA-binding affinity of GST-Ago2 and GST-D669A. Concentrations ranging from 3 nM to 300 nM of each recombinant protein were incubated with a fixed amount (10.8 nM) of 5′-^{32}P-radiolabeled-let-7a. The GST-Ago2:let-7a and GST-D669A:let-7a complexes were then analyzed by electrophoretic mobility shift assay (EMSA, Figure 2A and C). Using the Prism program, the dissociation constants (K_d) for GST-Ago2 and GST-D669A were determined to be 9.8 and 82.45 nM, respectively (Figure 2B and D). The higher dissociation constant of GST-D669A likely reflects the decreased RNA-binding affinity of the catalytically inactive protein.

Purified, Dicer-free, recombinant Ago2 does not process pre-miRNAs *in vitro*

We then sought to determine whether recombinant GST-Ago2 processes pre-miRNAs *in vitro*. We used recombinant human Dicer as positive control for the processing reactions. All preparations of GST-Ago2 protein prior to anion exchange chromatography tested positive for pre-miRNA processing (data not shown). We considered this activity to be a result of co-purification of endogenous Sf9 Dicer, which forms a stable complex with GST-Ago2. The pre-miRNA processing reactions proved a sensitive method to detect this complex. To dissociate Dicer from GST-Ago2, we purified the protein further using anion exchange chromatography. We monitored the purity of the protein by silver staining and tested the fractions using pre-miRNA processing and target RNA cleavage assays to assess Dicer and Ago2 activities, respectively. As shown in Figure 3, we identified fractions that were free of Dicer activity, but retained Ago2 activity. We used these purified, Dicer-free, GST-Ago2 fractions for all experiments described in the present work.

For pre-miRNA processing reactions, GST-Ago2, GST-D669A, or recombinant human Dicer was incubated with 5′-^{32}P-radiolabeled pre-let-7a-3. As expected, Dicer processed the pre-miRNA into an approximately 22 nt 5′-radiolabeled product (Figure 4A, lane 2). Dicer-free GST-Ago2 or GST-D669A did not show any pre-miRNA processing activity (Figure 4A, lanes 3 and 4).

Recombinant Ago2 and pre-miRNAs form active RISC complexes *in vitro*

We asked whether the complex of GST-Ago2 and Dicer would be sufficient to reconstitute active RLC *in vitro*, in the absence of TRBP. Combination of recombinant Dicer and GST-Ago2, *in vitro* in the presence of pre-let-7a-3 and 5′-^{32}P-radiolabeled target TD, generated a 5′-radiolabeled cleavage product of the expected size (Figure 4B, lane 2). This could suggest that TRBP was dispensable for *in vitro* reconstitution of mammalian RISC. However, unexpectedly, cleavage of target TD was also observed by purified, Dicer-free, GST-Ago2, but not GST-D669A, when Dicer was omitted from the reactions (Figure 4B, lane 4). Since Dicer was absent, and therefore pre-let-7a-3 was not processed into mature let-7a or any other detectable intermediate product, these results indicate that recombinant GST-Ago2 assembles with pre-let-7a-3 into a catalytically active complex.

Recombinant Ago2 forms catalytically active complexes with RNAs longer than miRNAs or siRNAs

In order to address if Ago2 can form complexes with pre-miRNAs, we first examined whether purified, Dicer-free, GST-Ago2 can bind to RNAs longer than miRNAs or siRNAs. We performed photo-crosslinking experiments of purified GST-Ago2 with 3′-^{32}P pCp radiolabeled RNAs. We used 70 nt pre-miRNA (either 5′-phosphorylated or non-phosphorylated pre-let-7a-3) or 73 nt unstructured single stranded RNA (ssRNA).

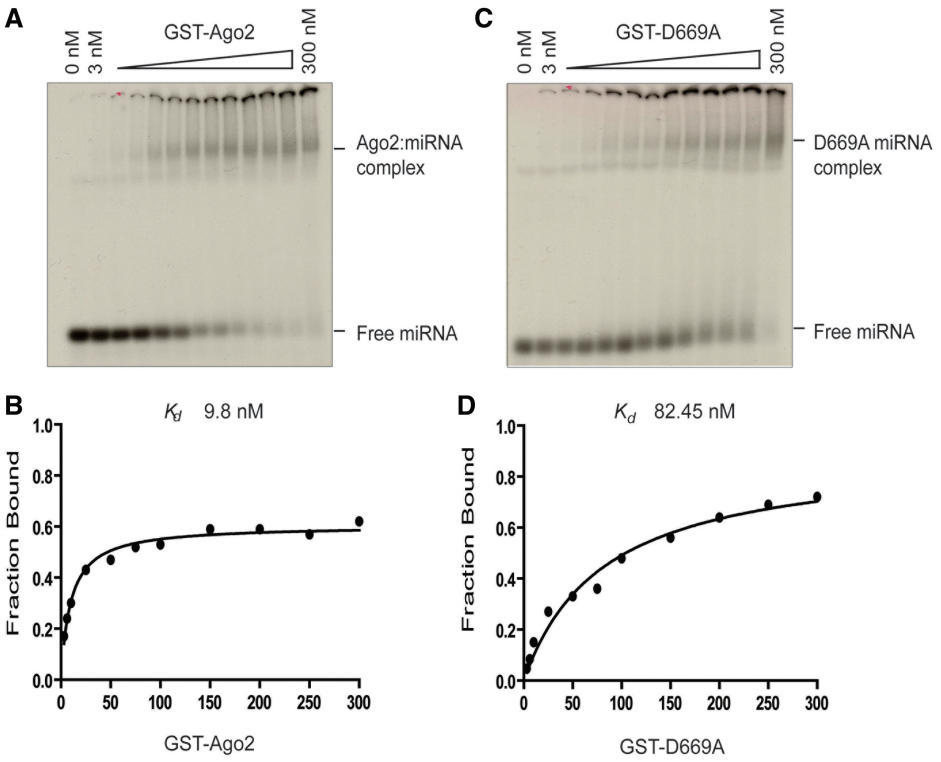

Figure 2. GST-Ago2:miRNA binding analysis. 5′-^{32}P-let-7a (10.8 nM) was incubated with increasing concentrations of GST-Ago2 or GST-D669A. GST-Ago2:let-7a (**A**) or GST-D669A:let-7a (**C**) complexes were analyzed by native gel electrophoresis. The fraction of let-7a bound to GST-Ago2 (**B**) or GST-D669A (**D**) was plotted against the concentration of the recombinant proteins. Panels show a representative of three independent experiments.

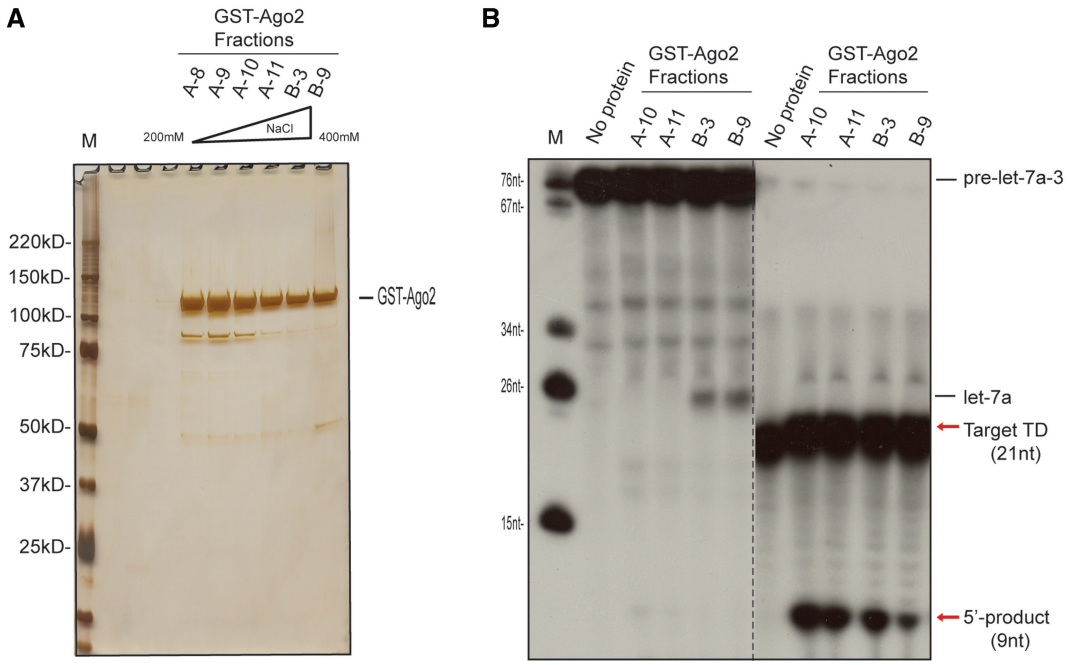

Figure 3. Endogenous Dicer activity from Sf9 cells co purifies with GST-Ago2. (**A**) Silver stained NuPAGE showing fractions obtained from anion exchange chromatography. GST-Ago2 was present in fractions with NaCl concentrations ranging from 200 to 400 mM. (**B**) GST-Ago2 containing fractions A10, A11, B3, and B9 were tested for pre-miRNA processing activity by incubation with 5′-^{32}P radiolabeled pre-let-7a-3. Reactions were then analyzed by 15% Urea PAGE and detected by autoradiography. Fractions A10 and A11 were Dicer-free. Cleavage of 5′-^{32}P-target TD by A10, A11, B3, and B9 fractions of purified GST-Ago2 pre-incubated with 5′P-let-7a. Reactions were analyzed on the same 15% Urea PAGE gel.

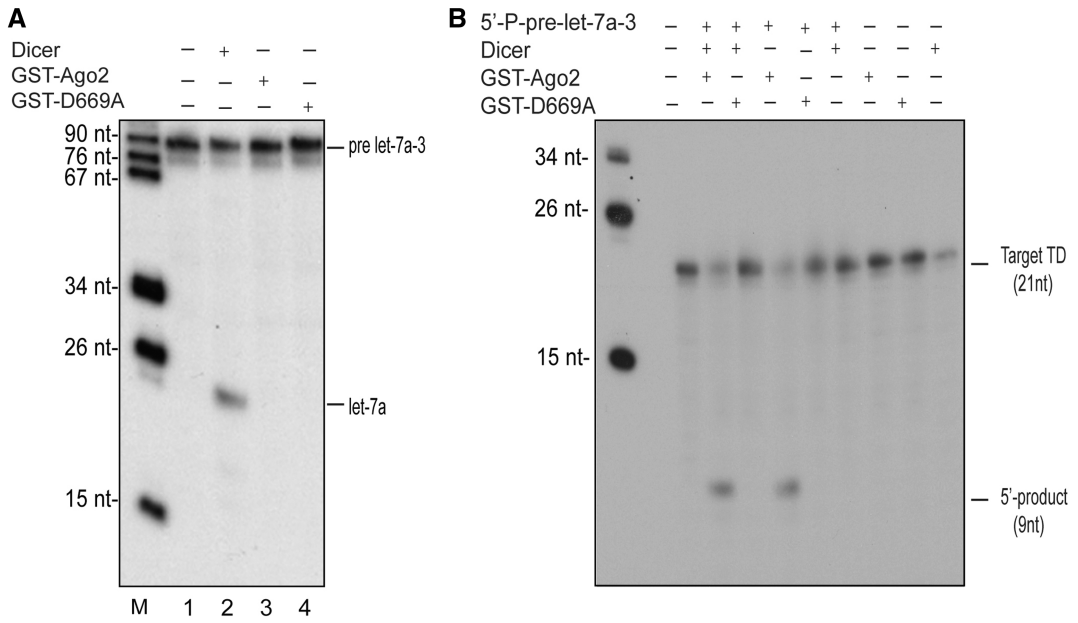

Figure 4. Purified, recombinant GST-Ago2 does not process pre-let-7a-3 *in vitro* and cleaves target TD in the absence of Dicer. (**A**) GST-Ago2, GST-D669A or recombinant human Dicer was incubated with 5′-^{32}P-pre-let-7a-3. Reaction products were analyzed by 15% Urea PAGE. (**B**) Purified, Dicer-free, GST-Ago2, GST-D669A or Dicer was pre-incubated with 5′P-pre-let-7a-3 before adding 5′-^{32}P target TD and analyzed by 15% Urea PAGE.

As controls, we used 22 nt miRNAs (5′-phosphorylated let-7a and non-phosphorylated let-7a). After ultraviolet (UV) crosslinking at 254 nm, the RNA-protein complexes were analyzed by NuPAGE and autoradiography. As shown in Figure 5A, purified, Dicer-free, GST-Ago2 bound to 5′-phosphorylated and non-phosphorylated pre-let-7a-3 as well as to unstructured 73 nt ssRNA. Competition by 10-, 50- and 100-fold molar excess of the corresponding unlabeled RNAs significantly reduced binding of GST-Ago2 to radiolabeled RNAs (Figure 5A), compared to the reactions where the same molar excess of nonspecific unlabeled yeast tRNA was used. These results indicate that recombinant GST-Ago2 can bind with high specificity to RNAs longer than miRNAs or siRNAs.

Next, we asked whether ribonucleoprotein complexes formed by GST-Ago2 and longer RNAs retained RISC activity. After loading purified, Dicer-free, GST-Ago2 with 5′-phosphorylated or non-phosphorylated pre-let-7a-3 or a 73 nt unstructured ssRNA, we performed *in vitro* cleavage reactions using a target RNA containing a sequence complementary to let-7a (TL). Nucleotides 1 to 21 of the 73 nt ssRNA have no similarity to the let-7a sequence (Figure 5C). As shown on Figure 5B, recombinant Ago2 bound to 5′P-pre-let-7a-3 or to 73 nt ssRNA cleaved the target TL, 10 nt across from the 5′-end of each guide RNA to produce a 46 nt or 60 nt cleavage product respectively. We also observed cleavage of a 33 nt RNA target TGS when GST-Ago2 was pre-loaded with gel purified 5′-phosphorylated pre-miR-30a (Supplementary Figure S4). A stronger signal of the same size, indicating an 18 nt 5′-cleavage product of target TGS was observed in control reactions where GST-Ago2 was pre-loaded with 5′-phosphorylated miR-30a but not when GST-Ago2 was free of RNAs (Supplementary Figure S4). Again, reactions where GST-Ago2 was incubated with 5′-^{32}P-radiolabeled pre-miR-30a showed that recombinant GST-Ago2 did not process pre-miR-30a into mature miR-30a (Supplementary Figure S4). These results indicate that, *in vitro*, recombinant GST-Ago2 forms active RISC complexes using as guides pre-miRNAs or unstructured single stranded RNAs longer than miRNAs or siRNAs.

Endogenous mammalian Ago2 associates with endogenous pre-miRNAs

Next, we asked whether the association of recombinant Ago2 with pre-miRNAs that we detected *in vitro* was also a property of endogenous human Ago2. Since Ago proteins associate and co-immunoprecipitate with Dicer (24–26), we first sought to immunopurify endogenous Ago2 free of Dicer. We carried out immunoprecipitations in HeLa cell lysates initially using a monoclonal antibody against Ago2 that also cross-reacts with Ago1, 3 and 4 (27). Results are shown in Supplementary Figures S2 and S3. When 4G8, a monoclonal antibody with specificity for human Ago2 (28) became available, we continued our experiments using this antibody. We found that stringent washes using Empigen detergent dissociated endogenous Dicer from endogenous Ago2. In order to monitor Dicer association and ensure Dicer-free preparations of endogenous Ago2, we carried out *in vitro* processing reactions, using 5′-radiolabeled pre-let-7a-3 (Figure 6B) or pre-miR-30a (Figure 9C and Supplementary Figure S2). We considered these reactions to be a more sensitive test to detect Dicer activity, than western blots, which are less sensitive than enzymatic

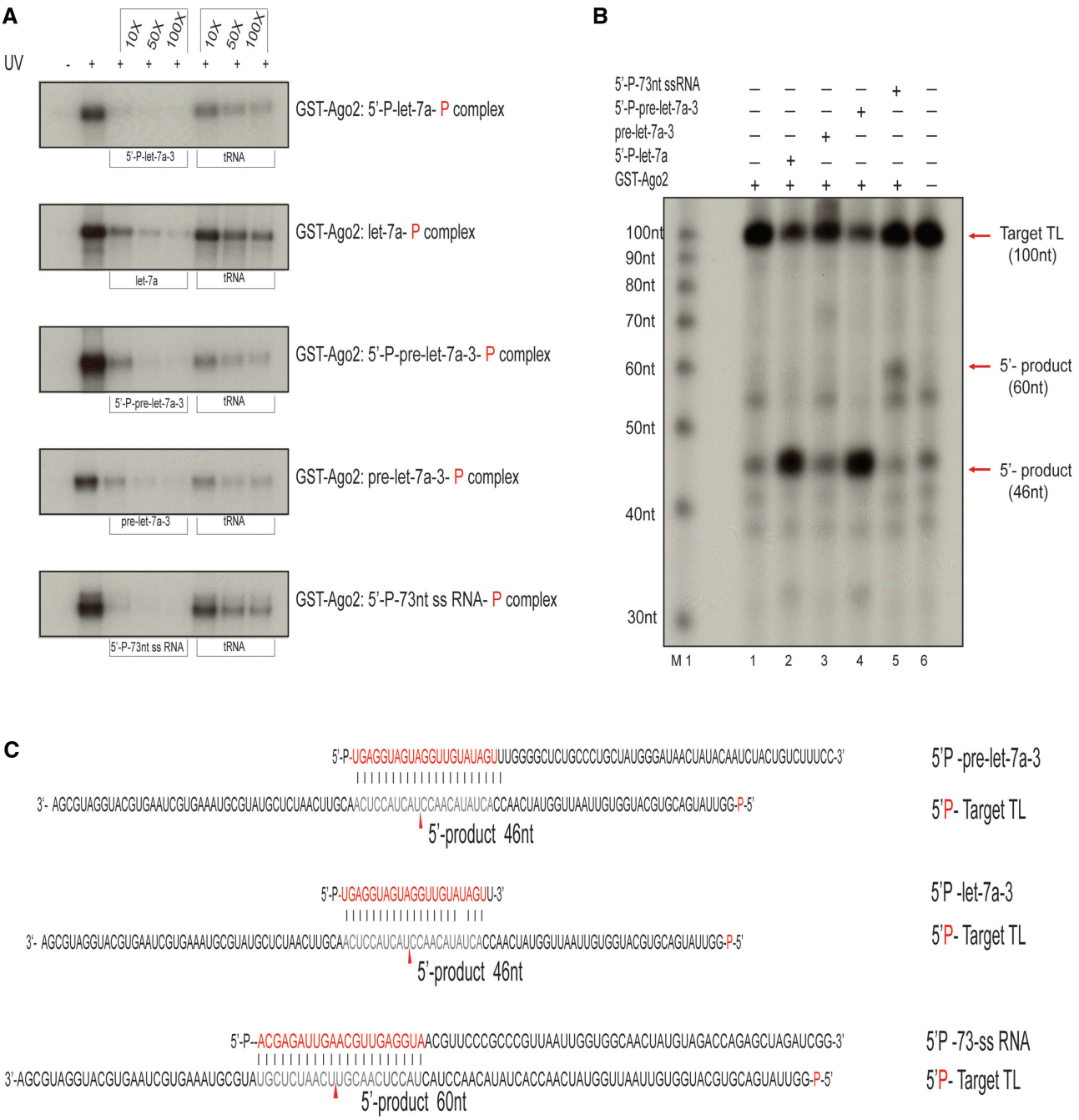

Figure 5. Purified, Dicer-free recombinant GST-Ago2 binds directly to pre-miRNAs or unstructured RNAs longer than miRNAs or siRNAs and forms active RISC. (**A**) A 2000 c.p.m. of 3′-^{32}P pCp labeled indicated RNA oligo was incubated with ~16.7 nM of recombinant, Dicer-free GST-Ago2, and then irradiated with 254 nM UV light. Photo-crosslinked samples were then analyzed by NuPAGE and detected by autoradiography. In competition experiments, 10×, 50× and 100× molar excess of unlabeled indicated RNA oligos or unlabeled tRNA were included. (**B**) 15 nM of GST-Ago2 was pre-incubated with 0.02 μM of 5′P-pre-let-7a-3, pre-let-7a-3, 5′P-73 nt unstructured single stranded RNA or mature 5′P-let-7a, followed by addition of 13.6 nmol 5′-^{32}P target TL (100 nt). Reaction products were analyzed by 10% Urea PAGE with Decade RNA size marker (M1) and detected by autoradiography. (**C**) Sequences of 5′P-pre-let-7a-3, 5′P-let-7a, 5′P-73 nt ssRNA oligo and target RNA (TL).

reactions. Washes with 0.5% Triton-containing solutions retained Dicer activity, whereas washes with 1% Empigen yielded immunoprecipitated endogenous Ago2 devoid of pre-miRNA processing activity (Supplementary Figure S2). We treated all preparations of endogenous human Ago2 with Empigen and assayed for pre-miRNA processing prior to performing any subsequent experiments. The presence of Ago2 in purified Empigen-treated agarose G beads was confirmed by western blotting (Figures 6A, 9B and Supplementary Figures S2B and S3B).

After confirming that neither binding to agarose G nor the catalytic activity of Ago2 was affected by Empigen treatment (data not shown), endogenous Ago2 was immunoprecipitated from HeLa cells under Empigen

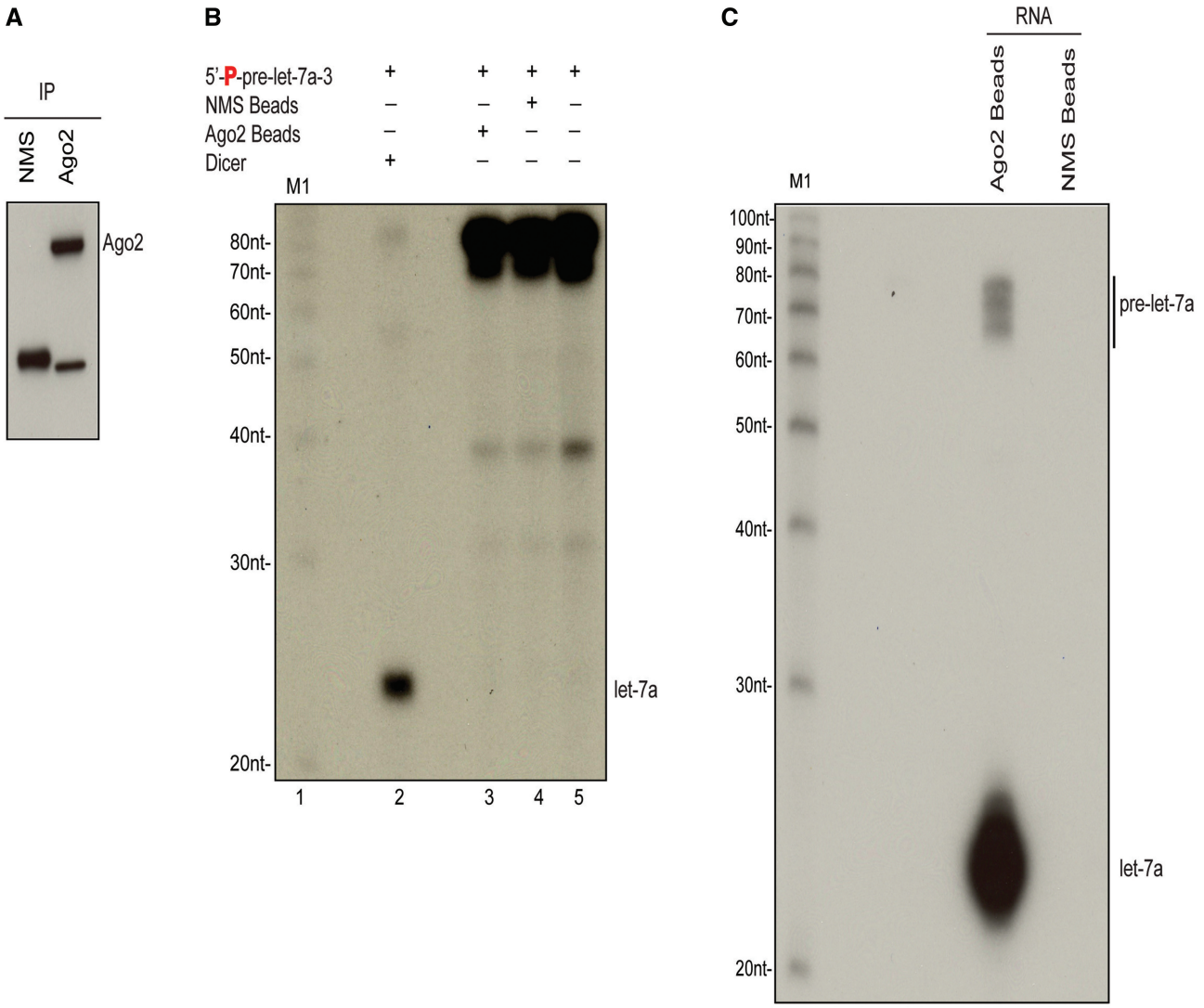

Figure 6. Endogenous human Ago2 binds directly to pre-let-7a-3. (**A**) Western blot of human Ago2 immunoprecipitates from total HeLa cell lysates. Non-immune mouse serum (NMS) was used as negative control. (**B**) Beads containing immunopurified Ago2 were washed with Empigen and then incubated with 5′-^{32}P-radiolabeled pre-let-7a-3. Recombinant Dicer and NMS were used as positive and negative controls for the processing reaction, respectively. (**C**) RNA isolated from immunopurified, Empigen-washed, Ago2 or from NMS was probed on Northern blot with an LNA probe against let-7a. The three distinct pre-let-7a signals correspond to the three isoforms of pre-let-7a (pre-let-7a-1, pre-let-7a-2 and pre-let-7a-3), detected by the LNA probe.

conditions, using the 4G8 antibody. Silver nitrate gel analysis and subsequent mass spectrometry were performed to ensure purity of the Ago2 immunoprecipitations (data not shown) before Ago2-bound RNA was isolated and subjected to northern blot analysis. The blots were probed with a locked nucleic acid-modified (LNA) probe against let-7a, a miRNA that is abundant in HeLa cells [(29) and our unpublished observations]. We detected a signal corresponding to pre-let-7a, along with the signal of mature let-7a (Figure 6C). In subsequent experiments, we used LNA probe for miR-21 and also detected binding of pre-miR-21 to endogenous human Ago2 (Figure 9D and data not shown). These findings indicate that, in addition to mature microRNAs, endogenous Ago2 directly associates with endogenous pre-miRNAs.

Accumulation of endogenous Ago:pre-miRNA complexes in the absence of Dicer

Our Ago2 immunoprecipitation and northern blot studies revealed that the precursors of two of the most abundant miRNAs in HeLa cells (miR-21 and let-7a) formed complexes with Ago proteins (Figure 6C, Supplementary Figure S3 and data not shown) and specifically with Ago2 (Figures 6C and 9D). We asked whether the abundance of Ago:pre-miRNA complexes increases in conditions where the processing of pre-miRNAs to mature miRNAs is blocked. Indeed, by immunoprecipitating with the 2A8 antibody and 3′-end labeling of endogenous Ago-bound RNAs from Dicer$^{-/-}$ MEFs, we demonstrated a significant enrichment of the Ago:pre-miRNA complexes in Dicer$^{-/-}$ MEFs, compared to

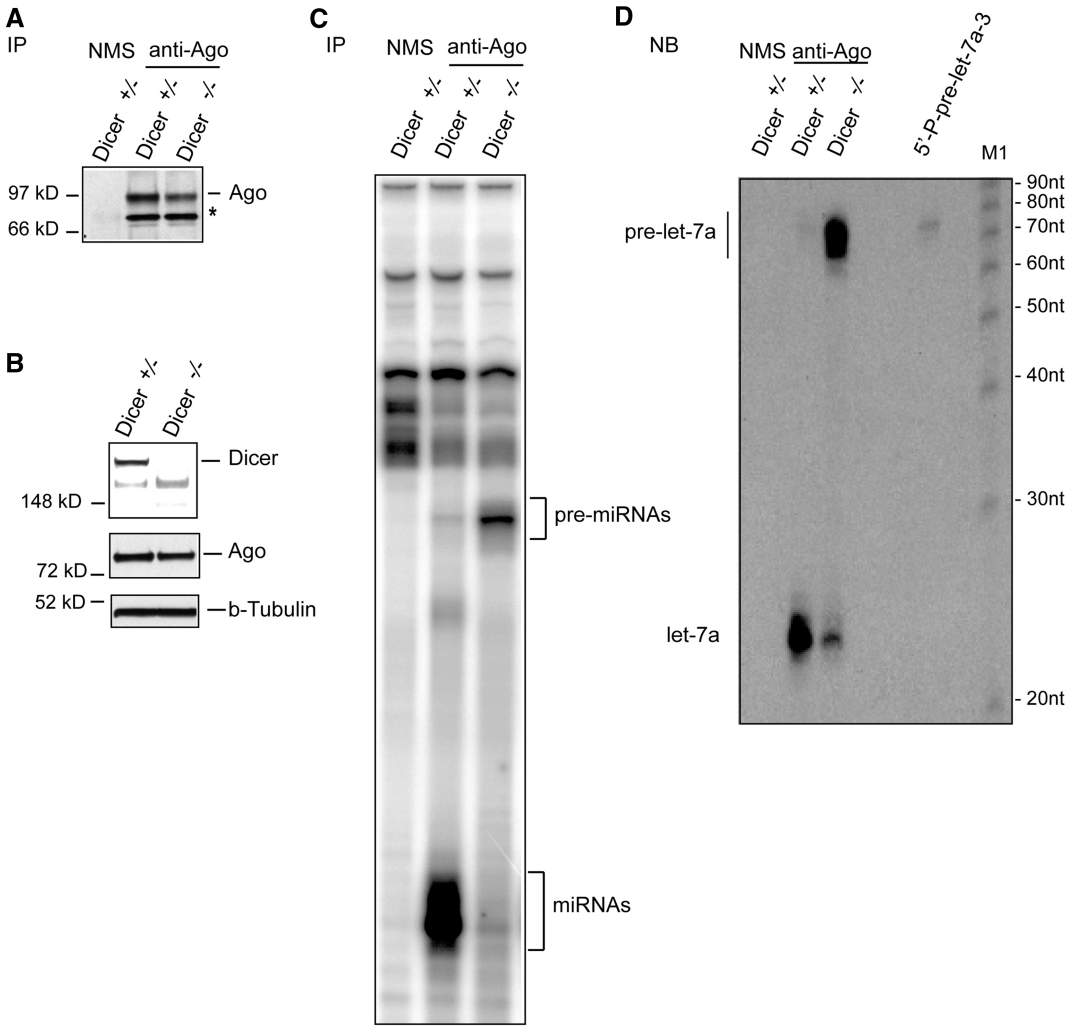

Figure 7. Accumulation of pre-miRNAs bound to Ago in Dicer-null mouse embryonic fibroblasts (MEFs). (**A**) Western blot showing similar amounts of Ago immunoprecipitated from *Dicer*$^{+/-}$ or *Dicer*$^{-/-}$ MEFs. The asterisk indicates cross-reaction of 2A8 antibody with radixin (27). (**B**) Western blots showing comparable expression of Agos in *Dicer*$^{+/-}$ and *Dicer*$^{-/-}$ MEFs and absence of Dicer in *Dicer*$^{-/-}$ MEF lysates. (**C**) RNA was isolated from Ago immunoprecipitated with anti-Ago 2A8 antibody or non-immune mouse serum (NMS) from *Dicer*$^{+/-}$ or *Dicer*$^{-/-}$ MEFs, 3′-end labeled with ^{32}P-pCp and resolved on a 15% Urea PAGE gel. Accumulation of pre-miRNAs concomitant with abrogation of miRNAs was detected in the anti-Ago IP from *Dicer*$^{-/-}$ MEFs. (**D**) Experiment was repeated as described in (**A–C**), except northern blot analysis of isolated RNA was performed and probed with LNA-let-7a. A total of 0.1 nM synthetic 5′P-pre-let-7a-3 was included as positive control.

Dicer$^{+/-}$ MEFs (Figure 7C). This observation was also confirmed through northern blot analysis with a LNA-let-7a probe, where a substantial increase in pre-let-7a signal bound to endogenous Ago was detected in Dicer-null MEFs, compared to Dicer$^{+/-}$ MEFs (Figure 7D). Minimal levels of mature miRNAs were detected in Ago immunoprecipitations from Dicer$^{-/-}$ MEFs. This is likely due to residual levels of mature miRNAs that are still detected after inducible deletion of Dicer and it may reflect stable mature miRNAs processed prior to the Dicer deletion. Enrichment of Ago:pre-miRNA complexes in Dicer$^{-/-}$ MEFs is not due to up-regulation of endogenous Ago proteins in MEFs in the absence of Dicer, since western blot studies on all MEF lysates as well as on 2A8-bound immunoprecipitated proteins, showed comparable levels of Agos between Dicer$^{-/-}$ and Dicer$^{+/-}$ (Figure 7A and B). These results demonstrate that Ago:pre-miRNA complexes accumulate in the absence of the pre-miRNA processing machinery.

Subcellular localization of endogenous human Ago2 and Ago2 ribonucleoprotein complexes

We then determined the localization of endogenous Ago2 in HeLa cells by immunofluorescence, using the Ago2-specific 4G8 monoclonal antibody (Figure 8B). We observed punctate cytoplasmic staining consistent with previous reports of Ago2 localization in cytoplasmic processing bodies (P-bodies) [Figure 8B and D; (28,30–32)]. We also observed diffuse cytoplasmic staining of endogenous Ago2 also consistent with previous reports (31,32). Furthermore, we found that endogenous Ago2 localizes also in the nucleus of HeLa cells (Figure 8B and D). Control experiments with either secondary

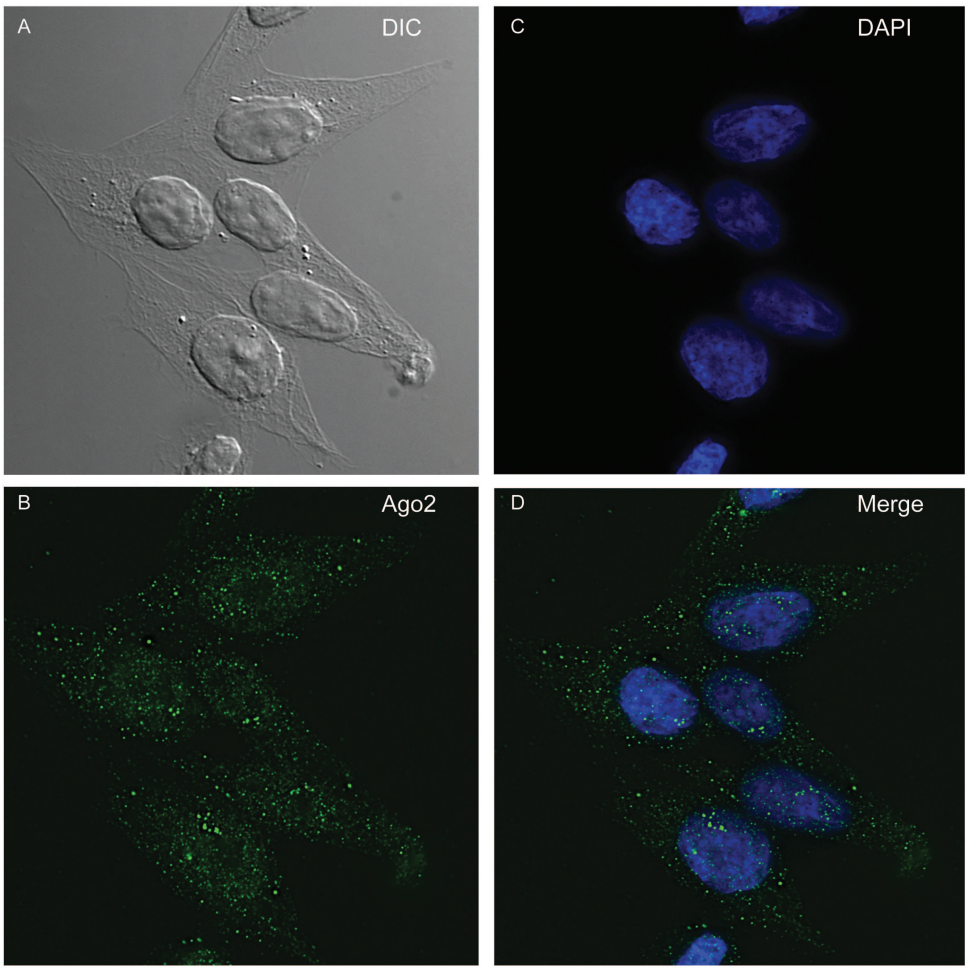

Figure 8. Endogenous human Ago2 is localized in the cytoplasm and nuclei of HeLa cells. (**A**) Differential interference contrast (DIC) image show the morphology of fixed and immunostained HeLa cells. (**B**) Endogenous Ago2 was immunostained with Ago2-specific antibody (4G8). The images were captured using deconvolution microscopy. (**C**) Nuclei of HeLa cells were co-stained with DAPI. (**D**) Merged images of (B) and (C), showing endogenous Ago2 in the cytoplasm and in the DAPI-stained nuclei.

antibody alone (Supplementary Figure S5A) or β-tubulin antibody (Supplementary Figure S5B) demonstrate specificity of endogenous Ago2 detection by 4G8.

Since we identified Ago2 in both nucleus and cytoplasm, we then investigated whether Ago2:pre-miRNA complexes are restricted to any of the two cellular compartments. To address this, we obtained fractions from HeLa cells enriched in nuclear or cytoplasmic components. We confirmed by western blot that Ago2 was present in both fractions (Figure 9A and Supplementary Figure S3A). Ago2 has been reported to associate with endoplasmic reticulum [ER (33,34)]. We tested whether components of the ER attached to the nuclear membrane, co-purified with the nuclear fractions. Western blot analysis using an antibody against the ER-associated protein calnexin showed that the nuclear fraction was essentially free of ER components (Figure 9A). Subsequently, we carried out Ago2 immunoprecipitations from nuclear and cytoplasmic fractions using the Ago2-specific 4G8 (Figure 9) or the monoclonal antibody 2A8 (Supplementary Figure S3). Ago2 binding to Empigen-treated agarose G beads was confirmed by western blot (Figure 9B and Supplementary Figure S3B). Processing reactions using 5′-radiolabeled pre-miR-30a or artificial PML-GL3 pre-miRNA (25) did not yield mature miRNA products, indicating that immunoprecipitated Empigen-treated endogenous Ago2 was Dicer-free (Figure 9C and Supplementary Figure S3C). Northern blot analysis of Ago2-bound RNA using a miR-21 LNA probe detected the presence of Ago2-bound pre-miR-21 primarily in nuclear fractions (Figure 9D). Ago2-bound pre-let-7a was detected in both nuclear and cytoplasmic fractions of 4G8 and 2A8 immunoprecipitated Ago2 (data not shown and Supplementary Figure S3D, respectively). We cannot comment on whether lower levels of precursors and mature miRNAs associated with cytoplasmic Ago2 reflect the actual levels of precursors and miRNAs in the two different cellular compartments or the effect of stringent washes with Empigen. Although this treatment resulted in dissociation of Dicer, we believe that some undesired loss of Ago2 and bound RNAs was unavoidable. Taken together, our results indicate that Ago2 and

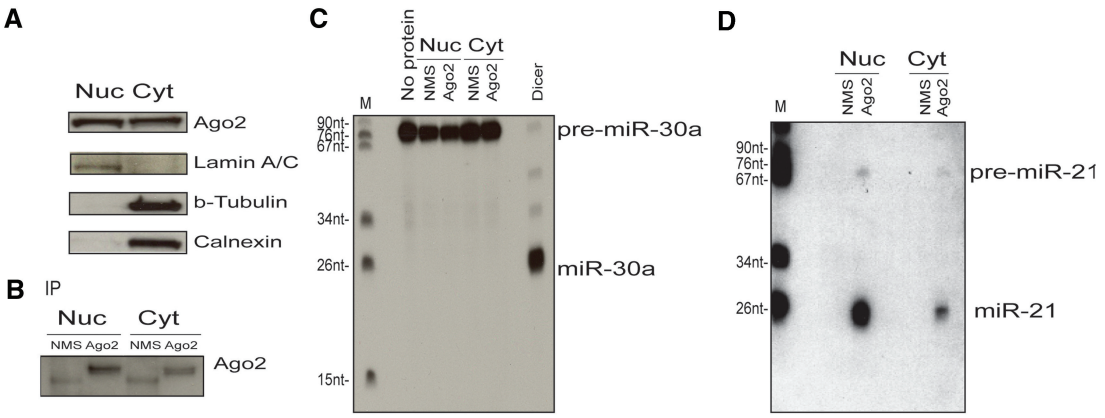

Figure 9. Nuclear and cytoplasmic human Ago2 associate with pre-miR-21. (A) Nuclear and cytoplasmic fractions of HeLa cells were probed on western blot with antibodies against indicated proteins. The same membrane was used with all antibodies. (B) Western blot of Ago2 immunoprecipitates from nuclear and cytoplasmic HeLa cell fractions. (C) Beads containing immunopurified Ago2 (or NMS) from nuclear and cytoplasmic fractions were washed with Empigen and then incubated with 5′-^{32}P-radiolabeled pre-miR-30a. Recombinant Dicer was used as positive control for the processing reaction. (D) RNA was isolated from nuclear and cytoplasmic Ago2 immunoprecipitates that had been washed with Empigen and probed on northern blot with an LNA probe against miR-21.

Ago2 ribonuclear complexes containing mature miRNAs and pre-miRNAs can be found in both nuclear and cytoplasmic compartments of human cells.

DISCUSSION

One of the objectives of our study was to characterize the RNA binding and nucleolytic activity of recombinant mammalian Ago2 in the absence of its binding partners. Cleavage kinetic analysis of human RISC, *Drosophila melanogaster* RISC (35) and reconstituted human RISC (36) has been previously studied (35–37). Recombinant human RISC loading complex (RLC) reconstitution by heterologous expression of human Dicer, Ago2 and TRBP in Sf9 cells and isolation of the three-protein complex by size exclusion chromatography has also been reported (38). With the exception of a study of recombinant human Ago2 generated in *Escherichia coli* by Rivas *et al.* (36), characterization studies of recombinant mammalian Ago2 have not been reported.

To ensure the purity of our preparations, after anion exchange chromatography, we performed activity assays to monitor for association of endogenous Sf9 Dicer with the recombinant mouse Ago2. It has been reported that endogenous human Ago2 cleaves certain pre-miRNAs to processing intermediates, termed Ago2-cleaved-precursors (ac-pre-miRNAs), by generating 10–12 nt nicked products. Our results indicate that recombinant Ago2 does not process pre-miRNAs *in vitro* as we did not detect mature miRNAs or any intermediate pre-miRNA processing products. This may suggest that, besides Ago2, other unknown factors that are required for generation of ac-pre-miRNAs were not present in our *in vitro* assays.

In RNA-binding studies with reconstituted human recombinant RISC loading complex (RLC) a K_d of 15 nM was previously reported for the complex of Ago2-Dicer-TRBP (38). We detected a higher RNA-binding affinity using recombinant Ago2, as reflected by a K_d of 9.8 nM. We also found that the K_d for the GST-D669A mutant is higher than that of wild-type Ago2, denoting less efficient miRNA binding of a catalytically inactive protein Ago2. The aspartate 669 is part of the Ago2 catalytic triad motif and is involved in coordinating metal ions vital for substrate cleavage activity (20). Our results from RNA-binding kinetic analyses of wild-type Ago2 and mutant GST-D669A suggest that metal ion coordination may also be critical for efficient RNA binding by Ago2.

The current paradigm states that Ago2 uses ~22 nt RNAs as guides for cleavage. Our study is the first to show that purified recombinant mammalian Ago2 binds miRNA precursors as well as unstructured RNAs longer than miRNAs or siRNAs. This binding is specific, as indicated by the competition UV crosslinking studies, and more importantly, results in the assembly of catalytically active Ago2 ribonucleoprotein complexes. In our studies, we have used several miRNA precursors, in addition to pre-let-7a and pre-miR-30a and we observed that recombinant Ago2 forms active complexes with all 5′-phosphorylated pre-miRNAs that we have tested so far (our unpublished data). We performed cleavage assays by pre-loading GST-Ago2 with pre-miRNAs or long unstructured RNA guides at concentrations ranging from 20 to 200 nM using approximately 16 nM of recombinant Ago2 protein and observed cleavage activity even with the lower pre-miRNA concentrations (our unpublished data). In order to avoid excess of unbound guide RNAs (pre-miRNAs or unstructured ssRNAs) in the cleavage reactions, we modified our protocol by using GST beads-bound recombinant GST-Ago2, which was washed stringently after loading with RNAs, before addition of the target RNA. We observed similar cleavage activity with this modified protocol (our unpublished data). The use by Ago2 of hairpin structured RNAs as guides to catalyze target RNA cleavage *in vitro* might be suggestive of RNA chaperone activity of Ago2, resulting in unwinding of the double stranded precursor stems or spontaneous unfolding of the precursors prior to

binding to their targets. Spontaneous basepair opening of double-stranded RNA as well as dissociation of RNA duplexes via strand displacement has been previously described (39,40).

In human cell lines, we observed that endogenous Ago2 also associates with endogenous pre-miRNAs. Using two different monoclonal antibodies that recognize human Ago2, we immunoprecipitated Dicer-free endogenous Ago2 from HeLa cells and showed by northern blot analyses, association with endogenous pre-let-7a and pre-miR-21. The ratio of pre-miRNAs to miRNAs bound to Ago2 reflects the ratio of pre-miRNAs to mature miRNAs in total RNA as detected previously by northern blot studies [(41) and our unpublished data] and most likely reflects the rapid processing of pre-miRNAs by Dicer. This is supported by our findings in Dicer-null cells where levels of pre-miRNAs associated to endogenous Ago2 increase significantly in the absence of Dicer, compared to wild-type cells, despite comparable expression of endogenous Ago2. Association of pre-miRNAs to Ago proteins has not been reported in previous studies, perhaps because of the lower sensitivity of the 3′-end labeling RNAs bound to immunoprecipitated Ago compared to the sensitivity of LNA probes. However in Dicer$^{-/-}$ cells where pre-miRNAs accumulate, we can clearly detect pre-miRNA association to Ago, by northern blot or even with 3′-end labeling of RNAs.

Our immunofluorescence studies performed in HeLa cells detected Ago2 in the cytoplasm and nucleus. The punctate cytoplasmic staining that we detected is consistent with previous reports of Ago2 localization in processing bodies (P-bodies) (28,30,31). We also detected nuclear Ago2, consistent with previous reports by recent studies showing Ago2 localization in the nuclei of human cells (32,42,43) and RISC activity in nuclear extracts of mammalian cells indicative of the presence of active Ago2:miRNA complexes in the nucleus (41,42). Results from our cell fractionation experiments correlate with our immunofluorescence studies confirming localization of Ago2 in the nucleus, in addition to the cytoplasm. Furthermore the presence of miR-21 in the nucleus has been previously reported (41,44). Although the role of Ago2 in the nucleus is not known, it has been previously reported that nuclear RNAi defective-3A (NRDE-3A), a *Caenorhabditis elegans* Ago protein, transports siRNAs from the cytoplasm to the nucleus (45). Evidence also exists for nuclear function of human Ago2 in transcriptional silencing by RNA duplexes targeting promoter sequences (46). Recently, a role for Importin 8 in the nuclear transport of human Ago2 has been reported (43).

In Ago2-null hematopoietic progenitor cells, fibroblasts and hepatocytes, miRNA microarrays revealed a several fold decrease in the abundance of mature miRNAs, suggestive of a role for Ago2 in the biogenesis of miRNAs (47). Since the decrease in mature miRNAs was not dependent on the catalytic activity of Ago2, it was suggested that Ago2 might increase access of pre-miRNAs to Dicer or increase Dicer's enzymatic activity (47). Our studies, which show direct association of endogenous human and mouse Ago2 to pre-miRNAs, may imply that Ago2 encounters miRNA precursors in the nucleus and cytoplasm at a step earlier than Dicer, perhaps facilitating access of pre-miRNAs to Dicer. This may explain why absence of Ago2 affects the abundance of mature miRNAs. The presence of mature miRNAs in the nucleus is also intriguing. If this is due to nuclear transport of miRNA-loaded Ago2 from the cytoplasm, as is the case for NRDE-3, or if pre-miRNA processing into mature miRNAs can also take place in the nucleus, remains to be determined.

In summary, our studies have uncovered a novel expanded RNA-binding activity of mammalian Ago2, by demonstrating that recombinant mouse Ago2 can use pre-miRNAs and RNAs longer than miRNAs as guides to cleave target RNAs, and that human and mouse Ago2 associates with pre-miRNAs *in vivo*. The biological implications of this novel finding will be the focus of future studies.

SUPPLEMENTARY DATA

Supplementary Data are available at NAR Online.

ACKNOWLEDGEMENTS

The authors are grateful to M. Siomi for 4G8 antibody, to V. N. Kim for anti-Dicer polyclonal antibody, to D. Schultz and the staff of the Protein Expression and Libraries Facility at the Wistar Institute for providing services and expertise and to David Metzler for technical support on protein purification.

FUNDING

National Institutes of Health/National Institute of Allergy and Infectious Diseases [K08AI063030 to M.K.]; the University of Pennsylvania [to M.K.] the National Institutes of Health/National Institute of Arthritis and Musculoskeletal and Skin Diseases [T32-AR007442-22 to B.G.G.] and the National Institutes of Health/National Institute of General Medical Sciences [R01GM080783 to M.T.M.]. Funding for open access charge: National Institutes of Health and University of Pennsylvania.

Conflict of interest statement. None declared.

REFERENCES

1. Mourelatos,Z., Dostie,J., Paushkin,S., Sharma,A., Charroux,B., Abel,L., Rappsilber,J., Mann,M. and Dreyfuss,G. (2002) miRNPs: a novel class of ribonucleoproteins containing numerous microRNAs. *Genes Dev.*, **16**, 720–728.
2. Hutvagner,G. and Zamore,P.D. (2002) A microRNA in a multiple-turnover RNAi enzyme complex. *Science*, **297**, 2056–2060.
3. Hammond,S.M., Boettcher,S., Caudy,A.A., Kobayashi,R. and Hannon,G.J. (2001) Argonaute2, a link between genetic and biochemical analyses of RNAi. *Science*, **293**, 1146–1150.
4. Vasudevan,S. and Steitz,J.A. (2007) AU-rich-element-mediated upregulation of translation by FXR1 and Argonaute 2. *Cell*, **128**, 1105–1118.

5. Kim,D.H., Saetrom,P., Snove,O. Jr and Rossi,J.J. (2008) MicroRNA-directed transcriptional gene silencing in mammalian cells. *Proc. Natl Acad. Sci. USA*, **105**, 16230–16235.
6. Wu,L. and Belasco,J.G. (2008) Let me count the ways: mechanisms of gene regulation by miRNAs and siRNAs. *Mol. Cell*, **29**, 1–7.
7. Kim,V.N., Han,J. and Siomi,M.C. (2009) Biogenesis of small RNAs in animals. *Nat. Rev. Mol. Cell Biol.*, **10**, 126–139.
8. Denli,A.M., Tops,B.B., Plasterk,R.H., Ketting,R.F. and Hannon,G.J. (2004) Processing of primary microRNAs by the Microprocessor complex. *Nature*, **432**, 231–235.
9. Han,J., Lee,Y., Yeom,K.H., Kim,Y.K., Jin,H. and Kim,V.N. (2004) The Drosha–DGCR8 complex in primary microRNA processing. *Genes Dev.*, **18**, 3016–3027.
10. Tomari,Y. and Zamore,P.D. (2005) MicroRNA biogenesis: drosha can't cut it without a partner. *Curr. Biol.*, **15**, R61–R64.
11. Yi,R., Qin,Y., Macara,I.G. and Cullen,B.R. (2003) Exportin-5 mediates the nuclear export of pre-microRNAs and short hairpin RNAs. *Genes Dev.*, **17**, 3011–3016.
12. Lund,E., Guttinger,S., Calado,A., Dahlberg,J.E. and Kutay,U. (2004) Nuclear export of microRNA precursors. *Science*, **303**, 95–98.
13. Kim,V.N. (2004) MicroRNA precursors in motion: exportin-5 mediates their nuclear export. *Trends Cell Biol.*, **14**, 156–159.
14. Bohnsack,M.T., Czaplinski,K. and Gorlich,D. (2004) Exportin 5 is a RanGTP-dependent dsRNA-binding protein that mediates nuclear export of pre-miRNAs. *RNA*, **10**, 185–191.
15. Lee,Y., Hur,I., Park,S.Y., Kim,Y.K., Suh,M.R. and Kim,V.N. (2006) The role of PACT in the RNA silencing pathway. *EMBO J.*, **25**, 522–532.
16. Kok,K.H., Ng,M.H., Ching,Y.P. and Jin,D.Y. (2007) Human TRBP and PACT directly interact with each other and associate with dicer to facilitate the production of small interfering RNA. *J. Biol. Chem.*, **282**, 17649–17657.
17. Zhang,H., Kolb,F.A., Jaskiewicz,L., Westhof,E. and Filipowicz,W. (2004) Single processing center models for human Dicer and bacterial RNase III. *Cell*, **118**, 57–68.
18. Kolb,F.A., Zhang,H., Jaronczyk,K., Tahbaz,N., Hobman,T.C. and Filipowicz,W. (2005) Human dicer: purification, properties, and interaction with PAZ PIWI domain proteins. *Methods Enzymol.*, **392**, 316–336.
19. Tahbaz,N., Kolb,F.A., Zhang,H., Jaronczyk,K., Filipowicz,W. and Hobman,T.C. (2004) Characterization of the interactions between mammalian PAZ PIWI domain proteins and Dicer. *EMBO Rep.*, **5**, 189–194.
20. Liu,J., Carmell,M.A., Rivas,F.V., Marsden,C.G., Thomson,J.M., Song,J.J., Hammond,S.M., Joshua-Tor,L. and Hannon,G.J. (2004) Argonaute2 is the catalytic engine of mammalian RNAi. *Science*, **305**, 1437–1441.
21. Kiriakidou,M., Nelson,P., Lamprinaki,S., Sharma,A. and Mourelatos,Z. (2005) Detection of microRNAs and assays to monitor microRNA activities *in vivo* and *in vitro*. *Methods Mol. Biol.*, **309**, 295–310.
22. Maniataki,E., De Planell Saguer,M.D. and Mourelatos,Z. (2005) Immunoprecipitation of microRNPs and directional cloning of microRNAs. *Methods Mol. Biol.*, **309**, 283–294.
23. Harfe,B.D., McManus,M.T., Mansfield,J.H., Hornstein,E. and Tabin,C.J. (2005) The RNaseIII enzyme Dicer is required for morphogenesis but not patterning of the vertebrate limb. *Proc. Natl Acad. Sci. USA*, **102**, 10898–10903.
24. Meister,G., Landthaler,M., Peters,L., Chen,P.Y., Urlaub,H., Luhrmann,R. and Tuschl,T. (2005) Identification of novel argonaute-associated proteins. *Curr. Biol.*, **15**, 2149–2155.
25. Maniataki,E. and Mourelatos,Z. (2005) A human, ATP-independent, RISC assembly machine fueled by pre-miRNA. *Genes Dev.*, **19**, 2979–2990.
26. Hock,J., Weinmann,L., Ender,C., Rudel,S., Kremmer,E., Raabe,M., Urlaub,H. and Meister,G. (2007) Proteomic and functional analysis of Argonaute-containing mRNA-protein complexes in human cells. *EMBO Rep.*, **8**, 1052–1060.
27. Nelson,P.T., De Planell-Saguer,M., Lamprinaki,S., Kiriakidou,M., Zhang,P., O'Doherty,U. and Mourelatos,Z. (2007) A novel monoclonal antibody against human Argonaute proteins reveals unexpected characteristics of miRNAs in human blood cells. *RNA*, **13**, 1787–1792.
28. Azuma-Mukai,A., Oguri,H., Mituyama,T., Qian,Z.R., Asai,K., Siomi,H. and Siomi,M.C. (2008) Characterization of endogenous human Argonautes and their miRNA partners in RNA silencing. *Proc. Natl Acad. Sci. USA*, **105**, 7964–7969.
29. Landgraf,P., Rusu,M., Sheridan,R., Sewer,A., Iovino,N., Aravin,A., Pfeffer,S., Rice,A., Kamphorst,A.O., Landthaler,M. *et al.* (2007) A mammalian microRNA expression atlas based on small RNA library sequencing. *Cell*, **129**, 1401–1414.
30. Chu,C.Y. and Rana,T.M. (2006) Translation repression in human cells by microRNA-induced gene silencing requires RCK/p54. *PLoS Biol.*, **4**, e210.
31. Leung,A.K., Calabrese,J.M. and Sharp,P.A. (2006) Quantitative analysis of Argonaute protein reveals microRNA-dependent localization to stress granules. *Proc. Natl Acad. Sci. USA*, **103**, 18125–18130.
32. Rudel,S., Flatley,A., Weinmann,L., Kremmer,E. and Meister,G. (2008) A multifunctional human Argonaute2-specific monoclonal antibody. *RNA*, **14**, 1244–1253.
33. Cikaluk,D.E., Tahbaz,N., Hendricks,L.C., DiMattia,G.E., Hansen,D., Pilgrim,D. and Hobman,T.C. (1999) GERp95, a membrane-associated protein that belongs to a family of proteins involved in stem cell differentiation. *Mol. Biol. Cell*, **10**, 3357–3372.
34. Tahbaz,N., Carmichael,J.B. and Hobman,T.C. (2001) GERp95 belongs to a family of signal-transducing proteins and requires Hsp90 activity for stability and Golgi localization. *J. Biol. Chem.*, **276**, 43294–43299.
35. Haley,B. and Zamore,P.D. (2004) Kinetic analysis of the RNAi enzyme complex. *Nat. Struct. Mol. Biol.*, **11**, 599–606.
36. Rivas,F.V., Tolia,N.H., Song,J.J., Aragon,J.P., Liu,J., Hannon,G.J. and Joshua-Tor,L. (2005) Purified Argonaute2 and an siRNA form recombinant human RISC. *Nat. Struct. Mol. Biol.*, **12**, 340–349.
37. Martinez,J. and Tuschl,T. (2004) RISC is a 5′ phosphomonoester-producing RNA endonuclease. *Genes Dev.*, **18**, 975–980.
38. MacRae,I.J., Ma,E., Zhou,M., Robinson,C.V. and Doudna,J.A. (2008) In vitro reconstitution of the human RISC-loading complex. *Proc. Natl Acad. Sci. USA*, **105**, 512–517.
39. Hart,K., Nystrom,B., Ohman,M. and Nilsson,L. (2005) Molecular dynamics simulations and free energy calculations of base flipping in dsRNA. *RNA*, **11**, 609–618.
40. Homann,M., Nedbal,W. and Sczakiel,G. (1996) Dissociation of long-chain duplex RNA can occur via strand displacement in vitro: biological implications. *Nucleic Acids Res.*, **24**, 4395–4400.
41. Meister,G., Landthaler,M., Patkaniowska,A., Dorsett,Y., Teng,G. and Tuschl,T. (2004) Human Argonaute2 mediates RNA cleavage targeted by miRNAs and siRNAs. *Mol. Cell*, **15**, 185–197.
42. Robb,G.B., Brown,K.M., Khurana,J. and Rana,T.M. (2005) Specific and potent RNAi in the nucleus of human cells. *Nat. Struct. Mol. Biol.*, **12**, 133–137.
43. Weinmann,L., Hock,J., Ivacevic,T., Ohrt,T., Mutze,J., Schwille,P., Kremmer,E., Benes,V., Urlaub,H. and Meister,G. (2009) Importin 8 is a gene silencing factor that targets argonaute proteins to distinct mRNAs. *Cell*, **136**, 496–507.
44. Hwang,H.W., Wentzel,E.A. and Mendell,J.T. (2007) A hexanucleotide element directs microRNA nuclear import. *Science*, **315**, 97–100.
45. Guang,S., Bochner,A.F., Pavelec,D.M., Burkhart,K.B., Harding,S., Lachowiec,J. and Kennedy,S. (2008) An Argonaute transports siRNAs from the cytoplasm to the nucleus. *Science*, **321**, 537–541.
46. Janowski,B.A., Huffman,K.E., Schwartz,J.C., Ram,R., Nordsell,R., Shames,D.S., Minna,J.D. and Corey,D.R. (2006) Involvement of AGO1 and AGO2 in mammalian transcriptional silencing. *Nat. Struct. Mol. Biol.*, **13**, 787–792.
47. O'Carroll,D., Mecklenbrauker,I., Das,P.P., Santana,A., Koenig,U., Enright,A.J., Miska,E.A. and Tarakhovsky,A. (2007) A Slicer-independent role for Argonaute 2 in hematopoiesis and the microRNA pathway. *Genes Dev.*, **21**, 1999–2004.